Chemically Induced Dynamic Electron Polarization Generated through the Interaction between Singlet Molecular Oxygen and Nitroxide Radicals

Claudia G. Martínez,[†] Steffen Jockusch,[†] Marco Ruzzi,[†] Elena Sartori,[†] Alberto Moscatelli,[†] Nicholas J. Turro,*[,†] and Anatoly L. Buchachenko[‡]

Department of Chemistry, Columbia University, New York, New York 10027, and N. N. Semenov Institute of Chemical Physics, Russian Academy of Sciences, Moscow, Russian Federation

Received: June 7, 2005; In Final Form: August 8, 2005

An absorptive chemically induced dynamic electron polarization (CIDEP) was generated by the quenching of singlet oxygen by nitroxide radicals (TEMPO derivatives). The spin polarization decay time of the nitroxide (measured by time-resolved EPR) correlates with the lifetime of singlet oxygen (measured by singlet oxygen phosphorescence spectroscopy). In addition, a deuterium isotope effect on the spin polarization decay time was observed, a signature of singlet oxygen involvement. With use of isotope labeled nitroxides (^{15}N, ^{14}N), the relative spin polarization efficiencies of TEMPO, 4-oxo-TEMPO, and 4-hydroxy-TEMPO by singlet oxygen were determined. The relative spin polarization efficiencies (per quenching event) decrease in the order 4-hydroxy-TEMPO > TEMPO > 4-oxo-TEMPO, whereas an opposite trend was observed for the total quenching rate constants of singlet oxygen by the nitroxides where the order is 4-hydroxy-TEMPO < TEMPO < 4-oxo-TEMPO.

Introduction

Chemically induced dynamic electron spin polarization (CIDEP) generated through the interaction of radicals, such as nitroxides, with triplet excited states of ketones or aromatic hydrocarbons has been studied extensively. The radical−triplet pair mechanism (RTPM) is the standard mechanistic description.[1−8]

Equations 1−10 represent a series of elementary steps that have been proposed to explain the CIDEP that is observed when anthracene is photoexcited in air-saturated solutions containing nitroxides. In the absence of oxygen, when triplet anthracene molecules are quenched by a nitroxide molecule, net emissive TR-EPR signals of the nitroxide are expected (eq 5). The quartet and doublet spin states of the radical−triplet pair mix with each other by zero-field splitting and hyperfine interactions. As a result of this mixing, the decay of the quartet state of the pair occurs with different rates to the different spin sublevels of the doublet ground pair. This process induces an emissive type CIDEP sometimes superposed by a weak emission/absorption multiplet type polarization.[2,6]

$$A \xrightarrow{h\nu} {}^1A^* \tag{1}$$

$${}^1A^* \rightarrow {}^3A^* \tag{2}$$

$${}^1A^* + {}^3O_2 \xrightarrow{k^{O_2}_{SA}} {}^3A^* + {}^1O_2 \tag{3}$$

$${}^3A^* \rightarrow A \tag{4}$$

$${}^3A^* + \text{O-TEMPO} \xrightarrow{k^{NO}_{qT}} A + (\text{O-TEMPO})^* \tag{5}$$

$${}^3A^* + {}^3O_2 \xrightarrow{k^{O_2}_{TA}} A + {}^1O_2 \tag{6}$$

$${}^1O_2 + \text{O-TEMPO} \xrightarrow{k^{NO}_{q\Delta}} {}^3O_2 + (\text{O-TEMPO})^* \tag{7}$$

$${}^1O_2 + A \xrightarrow{k^{A}_{q\Delta}} {}^3O_2 + A \tag{8}$$

$$(\text{O-TEMPO})^* \xrightarrow{k_{relax}} \text{O-TEMPO} \tag{9}$$

$${}^1O_2 \xrightarrow{k_\Delta} {}^3O_2 \tag{10}$$

In contrast to the emissive CIDEP signal from the nitroxide in the absence of oxygen, Obi et al. observed *absorptive* CIDEP of nitroxides in air-saturated solutions of nitroxides and triplet sensitizers, such as anthracene, naphthalene, and benzophenone.[9] This unusual absorption phase of the CIDEP was explained with the involvement of singlet oxygen $^1O_2$ ($^1\Delta_g$). Singlet oxygen is generated in air-saturated solutions by quenching of the triplet states of the sensitizer by triplet oxygen (eq 6). The triplet state of the sensitizer is generated by laser excitation of the sensitizer to form a singlet (eq 1) followed by intersystem crossing (eq 2). The radical−triplet pair mechanism (doublet precursor RTPM) explains the net absorptive CIDEP.[3,7] Enhanced intersystem crossing of $^1O_2$ to $^3O_2$ (eq 7), catalyzed by spin exchange interactions with the nitroxide, selectively yields the doublet spin states of radical−triplet pairs leading to an absorptive CIDEP.[9−13] In a recent paper by Obi et al. the magnitude of this net absorptive spin polarization of the nitroxide was estimated to be extraordinarily large (340 in the units of Boltzmann polarization).[13]

Given the unusual nature of the polarization and the complexity of the system (eqs 1−10), we decided to investigate the

[†] Columbia University.
[‡] Russian Academy of Sciences.

10.1021/jp0530404 CCC: $30.25
Published on Web 10/25/2005

CHART 1

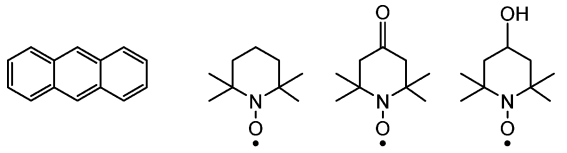

intermediacy of $^1O_2$ by standard tests such as the correlation of the CIDEP signals with known deuterium isotope effects on the lifetime of $^1O_2$ and the direct observation of the phosphorescence of $^1O_2$.[14] For our studies we selected anthracene as the singlet oxygen sensitizer and the three nitroxides, TEMPO, O-TEMPO, and OH-TEMPO (Chart 1). To obtain semiquantitative information about the polarization efficiency, we used mixtures of ^{14}N and ^{15}N isotope labeled nitroxides.

In addition to its inherent scientific interest, this work has relevance because of the involvement of nitroxides in polymer stabilizers. Hindered amines, such as tetramethylpiperidines, are widely used additives in paints and other polymer products as light stabilizers to delay polymer degradation.[15] The hindered amines scavenge polymer-damaging oxidizing intermediates, such as singlet oxygen and peroxides, and form stable nitroxide radicals. The nitroxide radicals, in turn, can act as additional quenchers of singlet oxygen or scavenge polymer radicals to form aminoethers, which can get reoxidized to nitroxides. The mechanism of polymer stabilization, using hindered amine light stabilizers (HALS), which involve nitroxide radicals, has been extensively studied.[15−19]

Experimental Section

Materials. Anthracene (Aldrich) was recrystallized from ethanol, and TEMPO (2,2,6,6-tetramethyl-1-piperidinyloxy) (Aldrich), O-TEMPO (4-oxo-2,2,6,6-tetramethyl-1-piperidinyloxy) (Aldrich), and OH-TEMPO (4-hydroxy-2,2,6,6-tetramethyl-1-piperidinyloxy) (Aldrich) were recrystallized from hexane. The solvents benzene (Aldrich, spectroscopic grade) and d_6-benzene (Cambridge Isotope Laboratories) were used as received. 5,10,15,20-Tetraphenyl-21*H*,23*H*-porphine (Aldrich) was used without further purification. The ^{15}N isotope labeled O-TEMPO (4-oxo-2,2,6,6-tetramethyl-1-piperidinyloxy) (^{15}N-O-TEMPO) was synthesized as described previously.[20] In all other experiments, where the nitrogen isotope is not specified, ^{14}N in its natural isotopic ratio was used.

EPR Experiments. TR-EPR experiments employed the pulses (308 nm, 10 ns) from a Lambda Physik Lextra 50 excimer laser, a Bruker ER 100D X-band EPR spectrometer, and a PAR boxcar averager and signal processor (models 4420 and 4402). Sample solutions were passed through a flat quartz flow cell (~0.3 mm thick) in a rectangular cavity (ER 4101 STE) of the EPR spectrometer. Further details are described elsewhere.[21,22] Decay kinetics of spin polarization were recorded on a digital oscilloscope (TDS 360, Tektronix). The 2D-TR-EPR spectra were obtained with use of a Bruker E580 X-band EPR spectrometer with a cylindrical cavity (ER 4103TM). The transient EPR signal, generated by laser excitation (308 nm, 10 ns), was collected just after the microwave bridge preamplifier (20 Hz − 400 kHz). Several transient EPR signals were digitized and averaged over a time window of 100 μs by a digital oscilloscope triggered on the laser pulse (LeCroy 9450A, 300 MHz, 400MS/s) at each of 240 definite magnetic field positions. The oscilloscope and the magnetic field advance were computer controlled by a home written LabView program. The data matrix was then processed by subtracting from each transient a weighted average of the off-resonance signals acquired at low and high magnetic field. The steady-state CW-EPR experiments were performed on a Bruker EMX EPR spectrometer.

TABLE 1: Quenching Rate Constants of Singlet Oxygen by Nitroxides ($k_{q\Delta}^{NO}$) and Relative Spin Polarization Efficiencies

nitroxide	$k_{q\Delta}^{NO}$ (M^{-1} s^{-1})[a]	relative spin polarization efficiency[b]
O-TEMPO	$(4.5 \pm 0.2) \times 10^5$	1
TEMPO	$(1.8 \pm 0.1) \times 10^5$	3 ± 1
OH-TEMPO	$(1.3 \pm 0.1) \times 10^5$	4 ± 1

[a] In benzene at 23°C. [b] Relative spin polarization efficiency per quenching event determined by TR-EPR with use of a mixture of the nitroxides ^{14}N-TEMPO and ^{15}N-O-TEMPO.

Singlet Oxygen Luminescence Spectroscopy. Singlet oxygen luminescence lifetimes were measured by using the pulses (308 nm, 10 ns) from a Lambda Physik Lextra 50 excimer laser, which excited the sample solutions in a 1 × 10 mm^2 quartz cell. The singlet oxygen phosphorescence at 1270 nm was collected and isolated with use of a lens and filter system (Interference filter; NB-170-010-B; Spectrogon) and focused into a NIR sensitive PMT (H9170−45; Hamamatsu). The photocurrent from the PMT was amplified (SR 560, Stanford Research Systems) and stored on a digital oscilloscope (TDS 360, Tektronix). The rates of quenching of singlet oxygen by the used nitroxides (eq 7) were determined by monitoring the singlet oxygen phosphorescence decay kinetic at 1270 nm at different nitroxide concentrations (0 to 10 mM). Singlet oxygen was produced by photosensitization with 5,10,15,20-tetraphenyl-21*H*,23*H*-porphine, which was excited with pulses (532 nm, 10 ns) from a Spectra Physics Nd:YAG laser. Stern−Volmer analysis of the phosphorescence decays yielded the quenching rate constants ($k_{q\Delta}^{NO}$, see Table 1) which are in agreement with published values for other solvents.[23,24]

The rate constants for the quenching of $^1O_2$ by nitroxides are collected in Table 1.

Results and Discussion

Laser flash photolysis of argon-saturated benzene solutions of anthracene (8.4 mM) and O-TEMPO (4 mM) affords an intense TR-EPR spectrum shown in Figure 1a. As expected from the standard RTPM, the CIDEP spectrum displays an emissive triplet with a ^{14}N hyperfine splitting of about 14 G, which is typical for nitroxides. However, as reported[9−13] for air-saturated solutions containing the same concentrations of anthracene and O-TEMPO an absorptive TR-EPR spectrum was observed (Figure 1b). On the other hand, the TR-EPR spectrum was very weak when oxygen-saturated solutions were employed (Figure 1c).

Steady-state EPR spectra of the above solutions (argon, air, and oxygen-saturated benzene solutions of anthracene and O-TEMPO) were recorded employing the same experimental parameters (Figure 1d−f). Argon-saturated solutions show the typical narrow-line triplet with a ^{14}N hyperfine splitting of 14.3 G (Figure 1d). In air-saturated solution the three nitroxide lines are significantly broadened due to Heisenberg spin exchange with triplet molecular oxygen (Figure 1e).[25,26] In oxygen-saturated benzene solution the EPR spectrum of O-TEMPO is broadened by oxygen to an extent that it can be seen only after amplification (Figure 1f). This broadening explains the apparent absence of a TR-EPR signal in the oxygen-saturated solutions (Figure 1c): Heisenberg exchange broadening causes the signal to be broadened to the point it is difficult to detect in the TR-EPR.

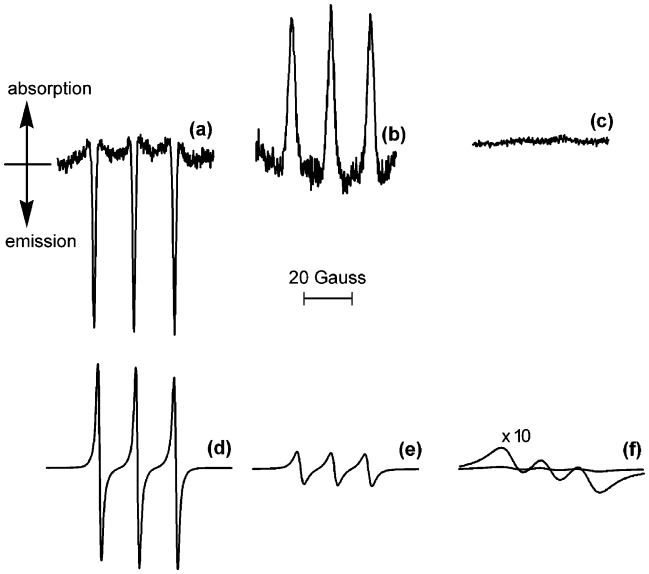

Figure 1. Time-resolved EPR spectra (a−c) recorded from 1 to 2 μs following laser excitation (308 nm, 10 ns) and steady-state EPR spectra (d−f) of anthracene (8.4 mM) and ^{14}N-O-TEMPO (4 mM) in argon (a, d), air (b, e), and oxygen (c, f) saturated benzene solution at 23 °C.

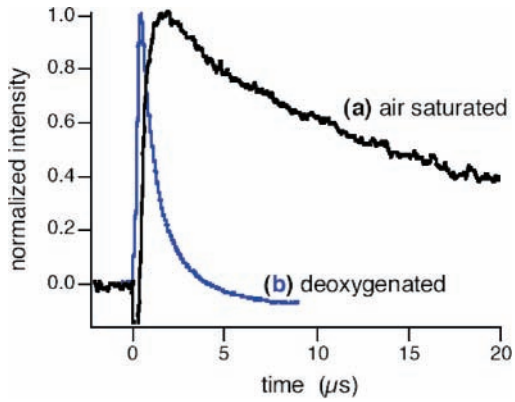

Figure 2. Transient EPR decay kinetic of the low-field hyperfine line of the nitroxide (3463 G) following laser excitation (308 nm, 10 ns) of anthracene (8.4 mM) and ^{14}N-O-TEMPO (4 mM) in argon (b) and air (a) saturated benzene solution. Decay trace a was inverted for convenient comparison with trace b.

Figure 2 shows the decay kinetics of the CIDEP signal of TEMPO in argon-saturated (b) and air-saturated (a) benzene solution. The decay time ($\tau \sim 1$ μs) of the emissive CIDEP signal in argon-saturated solutions (b) is significantly shorter than the decay time ($\tau \sim 27$ μs) of the absorptive CIDEP signal in air-saturated solutions (a). Under deoxygenated conditions the emissive CIDEP signal of O-TEMPO is generated by radical−triplet pair mechanism[1,2,4−6,8] involving O-TEMPO and the triplet state of anthracene. The triplet state of anthracene is generated by excitation (308 nm laser pulses) of anthracene (eq 1) and intersystem crossing (eq 2). The triplet state of anthracene is known to be quenched by TEMPO (eq 5) with a rate constant of $k_{qT}^{NO} = 1.2 \times 10^7$ M^{-1} s^{-1}.[9] The lifetime of the CIDEP signal of O-TEMPO (Figure 2b; $\tau \sim 1$ μs) is longer than the published relaxation time (T_1) for nitroxides (eq 9) (250−350 ns)[6,8,27] because it also depends on the anthracene triplet lifetime.

In air-saturated solutions the anthracene triplets are predominantly quenched by molecular triplet oxygen (eq 6) instead of by O-TEMPO (eq 5), because of the high quenching rate constant ($k_{T\Delta}^{O_2} = 3.4 \times 10^9$ M^{-1} s^{-1})[28] and high oxygen concentration dissolved in benzene (1.9 mM).[29] In this process (eq 6) singlet oxygen is generated quantitatively.[28,30,31] Furthermore, singlet oxygen can be generated by the quenching of singlet excited states of anthracene derivatives by triplet oxygen (eq 3). This process produces triplet anthracene (eq 3) that can in turn generate another singlet oxygen molecule (eq 6). Therefore, singlet oxygen quantum yields up to 1.12 (depending on the oxygen concentration) have been reported for sensitization with anthracene in benzene solutions.[30] Other reports showed that singlet oxygen production from the quenching of singlet excited states of anthracene by triplet oxygen (eq 3) is negligible.[28,31] Singlet oxygen is quenched by O-TEMPO (eq 7) with a rate constant of $k_{q\Delta}^{NO} = 4.5 \times 10^5$ M^{-1} s^{-1} (Table 1). Obi et al. attributed the absorptive CIDEP to this interaction of singlet oxygen with O-TEMPO.[9] If singlet oxygen is involved, the decay time of the CIDEP signal (Figure 1b) should be governed by the lifetime of singlet oxygen, because the relaxation time (T_1) for nitroxides (250−350 ns)[6,8,27] is much shorter than the lifetime of singlet oxygen in benzene. The singlet oxygen lifetime in pure benzene is reported to be 30 μs.[32] However, the lifetime under our experimental conditions is expected to be shorter, because of quenching of singlet oxygen by O-TEMPO and anthracene.[33] Therefore, we determined the singlet oxygen lifetime, employing a direct method, in the same sample solutions, which were also used for TR-EPR experiments. Singlet oxygen possesses a phosphorescence centered at 1270 nm,[14] which was used as an analytical tool to determine its lifetime. Figure 3b shows the singlet oxygen phosphorescence decay kinetic ($\tau_p = 25 \pm 2$ μs) recorded after laser excitation (308 nm) together with the decay kinetic of the CIDEP signal of O-TEMPO. Because both decay kinetics, singlet oxygen phosphorescence (Figure 3b) and CIDEP signal (Figure 3a), are very similar, we concluded that the lifetime of singlet oxygen determines the decay time of the CIDEP signal of O-TEMPO.

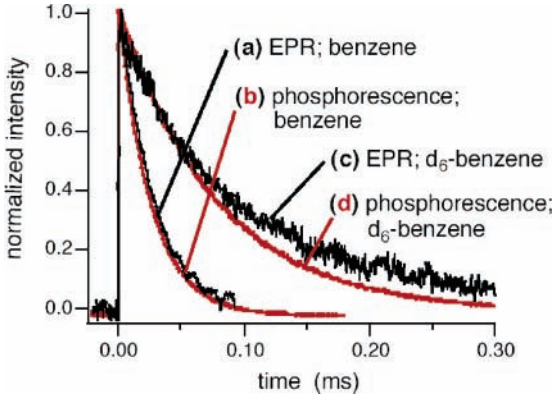

Figure 3. Singlet oxygen phosphorescence decay kinetic monitored at 1270 nm (b, d) and transient EPR decay kinetic of the low-field hyperfine line of the nitroxide (3464 G) (a, c) following laser excitation (308 nm, 10 ns) of anthracene (8.4 mM) and ^{14}N-O-TEMPO (4 mM) in air saturated benzene (a, b) and d_6-benzene (c, d) solution.

An increase of the singlet oxygen lifetime should also cause an increase in the decay time of the CIDEP signal. An excellent way to extend the lifetime of $^1O_2$ (eq 10) without modifying the other steps in eqs 1−9 significantly is to run the reaction in a deuterated solvent. For example, in pure perdeuterated benzene (d_6-benzene) a singlet oxygen lifetime of 681 μs is reported whereas a lifetime of the order of 30 μs is reported in h_6-benzene.[32] TR-EPR experiments on anthracene/O-TEMPO solutions were performed both in h_6-benzene and in d_6-benzene and the CIDEP decays are shown in Figure 3. A significantly longer decay time of the CIDEP signal was observed in d_6-benzene (Figure 3c; $\tau = 88 \pm 10$ μs) compared to nondeuterated benzene (Figure 3a; $\tau = 27 \pm 5$ μs). This strong deuterium effect is a signature of the involvement of singlet oxygen, whose

SCHEME 1: Reaction of O-TEMPO with Photoexcited Anthracene in the Presence of Oxygen

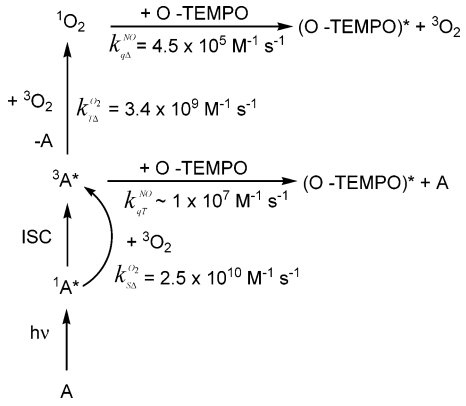

lifetime possesses an extraordinary dependence on the occurrence of CH versus CD bonds in the solvent.[34−36] The singlet oxygen lifetime in d_6-benzene under our experimental conditions ([anthracene] = 8.4 mM and [O-TEMPO] = 4 mM) was directly determined by time-resolved phosphorescence spectroscopy (λ_{ex} = 308 nm) and found to be $\tau_p = 78 \pm 4$ μs (Figure 3d), which is significantly shorter than in pure d_6-benzene (681 μs)[32] because of the quenching of singlet oxygen by O-TEMPO (eq 7), anthracene (eq 8), and possible impurities. Both decay kinetics, singlet oxygen phosphorescence (Figure 3d) and CIDEP signal (Figure 3c), are very similar.

Scheme 1 summarizes the important reactions and known rate constants involved in the anthracene/O-TEMPO system. After laser excitation, singlet excited states of anthracene (^{1}A*) are generated (eq 1), which can be quenched by molecular oxygen (triplet oxygen, $^3O_2$), $k_{S\Delta}^{O_2} = 2.5 \times 10^{10}$ M^{-1} s^{-1} (eq 3).[28] The triplet state of anthracene is generated by intersystem crossing (eq 2). The triplet anthracene (^{3}A*) can be quenched either by O-TEMPO (eq 5) (leading to emissive nitroxide CIDEP) or by molecular oxygen (triplet oxygen, $^3O_2$) to generate singlet oxygen ($^1O_2$) (eq 6). Which reaction dominates is determined by the bimolecular rate constants (k_{qT}^{NO} and $k_{T\Delta}^{O_2}$) and by the concentrations ([O-TEMPO] and [$^3O_2$]). Because the quenching rate constant ($k_{qT}^{NO} = 1.2 \times 10^7$ M^{-1} s^{-1})[9] of ^{3}A* by TEMPO is relatively low (2 orders of magnitude lower than for quenching of ketone triplets such as xanthone: $k_{T\Delta}^{O_2} = 8.9 \times 10^9$ M^{-1} s^{-1}),[37] singlet oxygen is generated efficiently by the quenching of ^{3}A* with $^3O_2$. Moreover, quenching of singlet excited states of anthracene by triplet oxygen can generate additional singlet oxygen (eq 3).

To increase the singlet oxygen yield (and consequently increase the CIDEP from $^1O_2$/O-TEMPO interactions) the concentration of molecular oxygen in benzene was increased by saturation of the benzene solutions with oxygen ([$^3O_2$] = 9.0 mM)[29] prior to the TR-EPR experiments. However, no CIDEP of O-TEMPO was observed in oxygen-saturated benzene solutions (Figure 1c). As mentioned earlier, the steady-state EPR of the same solution showed that the three-line nitroxide EPR spectrum is extensively broadened (Figure 1f) due to Heisenberg exchange with $^3O_2$.[25,26] Therefore, a high oxygen concentration causes a loss of the CIDEP signal. The line broadening due to oxygen in TR-EPR experiments was investigated systematically. The half-widths of the O-TEMPO spin polarized signal for oxygen concentrations of 0, 0.45, 1.9, and 4.5 mM are 1.2, 1.4, 3.3, and 4.6 G, respectively. These half-widths (TR-EPR) are in agreement with the half-width that we observed for O-TEMPO in Boltzmann distribution (steady-state EPR). The best CIDEP signal (best signal-noise ratio) for O-TEMPO polarization by singlet oxygen was observed at an oxygen concentration of 0.45 mM (saturation of the benzene solution with a 5% mixture of $^3O_2$ in N_2). The small loss in overall signal intensity (integrated signal) due to less efficient $^1O_2$ production (eq 6) is well compensated by the narrower lines.

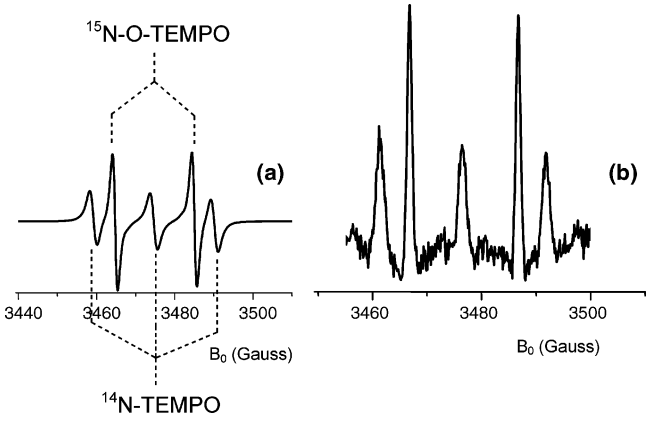

Figure 4. Steady-state EPR spectrum (a) and time-resolved EPR spectrum recorded from 1 to 2 μs following laser excitation (308 nm, 10 ns) (b) of benzene solutions of anthracene (8.4 mM), ^{14}N-TEMPO (2 mM), and ^{15}N-O-TEMPO (2 mM) in the presence of 0.45 mM oxygen at 23 °C.

Another parameter, which can be varied to improve the absorptive CIDEP due to $^1O_2$ interaction with O-TEMPO, is the concentration of O-TEMPO. An increase in the O-TEMPO concentration increases the rate of both reactions, ^{3}A* quenching by O-TEMPO (eq 5) (reduces CIDEP due to $^1O_2$ interaction with O-TEMPO) and $^1O_2$ quenching by O-TEMPO (eq 7) (increases CIDEP due to $^1O_2$ interaction with O-TEMPO) (Scheme 1). Because of the quenching rate constant k_{qT}^{NO} is 2 orders of magnitudes lower than $k_{T\Delta}^{O_2}$, ^{3}A* quenching by O-TEMPO can be neglected in air-saturated solutions. On the other hand, at a too high concentration of O-TEMPO Heisenberg spin exchange interactions between two nitroxides cause an EPR line broadening and consequently, again a loss of CIDEP signal. We chose an O-TEMPO concentration of 4 mM, because at a higher concentration spin−spin interactions between the nitroxides were dominant.

The quenching rate constant of $^1O_2$ by nitroxides ($k_{q\Delta}^{NO}$) depends on the structure of the nitroxide (Chart 1, Table 1). O-TEMPO shows a higher quenching rate constant of $^1O_2$ ($k_{q\Delta}^{NO} = 4.5 \times 10^5$ M^{-1} s^{-1}) compared to TEMPO ($k_{q\Delta}^{NO} = 1.8 \times 10^5$ M^{-1} s^{-1}). Therefore, one could expect a stronger CIDEP signal from O-TEMPO compared to TEMPO (Scheme 1). To investigate nitroxide structure effects in detail we used an isotope labeled ^{15}N-O-TEMPO. Because ^{15}N possesses a spin multiplicity of $^1/_2$, in contrast to the spin multiplicity of ^{14}N of 1, both nitroxide spectra are readily distinguishable from each other.[38] TR-EPR experiments of equimolar amounts of ^{15}N-O-TEMPO and ^{14}N-TEMPO (2 mM) and anthracene (8.4 mM) were performed in the presence of 0.45 mM oxygen. An absorptively polarized TR-EPR spectrum consisting of 5 lines was observed, where the first, third, and fifth lines correspond to ^{14}N-TEMPO and the second and fourth lines to ^{15}N-O-TEMPO (Figure 4). Figure 5 shows the 2D-TR-EPR spectrum containing both spectral and kinetic information. The decay times of both spectral components ^{14}N-TEMPO and ^{15}N-O-TEMPO are identical within experimental error. Integration of the TR-EPR signals of ^{15}N-O-TEMPO and ^{14}N-TEMPO polarized by $^1O_2$ (Figure 4b) revealed a ratio of the intensities of approximately 1. This is in contrast to the ratio of the quenching rate constant of $^1O_2$ by O-TEMPO ($k_{q\Delta}^{NO} = 4.5 \times 10^5$ M^{-1} s^{-1}) and TEMPO

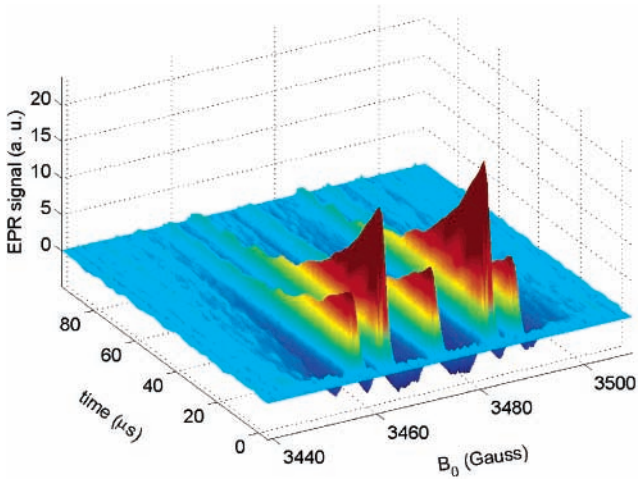

Figure 5. 2D-TR-EPR spectrum following laser excitation (308 nm, 10 ns) in benzene solutions of anthracene (8.4 mM), ^{14}N-TEMPO (2 mM), and ^{15}N-O-TEMPO (2 mM) in the presence of 0.45 mM oxygen at 23 °C.

($k_{q\Delta}^{NO} = 1.8 \times 10^5$ M^{-1} s^{-1}) of 2.6. Considering the observed polarization intensity ratio for ^{15}N-O-TEMPO and ^{14}N-TEMPO of approximately 1 (Figure 4b) and the ratio of the quenching constants of $^1O_2$ by the nitroxides, we conclude that the net absorptive spin polarization efficiency for TEMPO is significantly higher (approximately 3 ± 1 times that of O-TEMPO).

An alternative explanation for the observed equal intensities of the CIDEP signals for ^{14}N-TEMPO and ^{15}N-O-TEMPO is spin polarization transfer. If spin polarization transfer between the different nitroxide derivatives is fast enough to compete with the polarization relaxation, then it could also generate the observed CIDEP in Figures 4 and 5. However, experiments comparing the absolute CIDEP intensity of ^{14}N-TEMPO and ^{14}N-O-TEMPO separately (solution 1: [^{14}N-TEMPO] = 4 mM, [A] = 8.4 mM, [O_2] = 1.9 mM; solution 2: [^{14}N-O-TEMPO] = 4 mM, [A] = 8.4 mM, [O_2] = 1.9 mM) showed that also approximately equal CIDEP was observed. This does not rule out that the spin polarization transfer mechanism from one nitroxide to the other nitroxide derivative might have some contribution, but shows that direct polarization for all investigated nitroxides by singlet oxygen occurs.

A change of the concentration ratio of ^{14}N-TEMPO to ^{15}N-O-TEMPO should be directly reflected in the CIDEP ratios. Indeed, using 4 mM ^{14}N-TEMPO and 1 mM ^{15}N-O-TEMPO (concentration ratio = 4) generates a CIDEP ratio (TEMPO/O-TEMPO) of approximately 4.

Control experiments with equimolar amounts of ^{15}N-O-TEMPO and ^{14}N-O-TEMPO (2 mM) and anthracene (8.4 mM) in the presence of 0.45 mM oxygen showed that CIDEP signals of ^{15}N-O-TEMPO and ^{14}N-O-TEMPO of equal intensity (integrated signal intensity) were produced (within experimental error) demonstrating that our integration procedure is accurate.

OH-TEMPO quenches singlet oxygen significantly slower ($k_{q\Delta}^{NO} = 1.3 \times 10^5$ M^{-1} s^{-1}) than O-TEMPO ($k_{q\Delta}^{NO} = 4.5 \times 10^5$ M^{-1} s^{-1}). However, TR-EPR experiments with equimolar amounts of ^{15}N-O-TEMPO and ^{14}N-OH-TEMPO (2 mM) and anthracene (8.4 mM) in the presence of 0.45 mM oxygen showed again CIDEP signals of ^{15}N-O-TEMPO and ^{14}N-OH-TEMPO of similar intensity.

It is noteworthy to mention that for the experiments involving mixtures of ^{15}N and ^{14}N labeled nitroxides a low oxygen concentration (0.45 mM) was used to be able to resolve the EPR lines of ^{15}N and ^{14}N for accurate integration. A higher oxygen concentration would broaden the five nitroxide lines due to Heisenberg spin exchange and cause an overlap between the ^{15}N and ^{14}N lines.

A possible explanation of the differences between the effectiveness of the quenching of singlet oxygen by nitroxides and the polarization of nitroxides by singlet oxygen hypothesizes that the polarization mechanism is only active over a small range of the nitroxide structure near the N−O group, whereas quenching is active over the entire molecule. In this scenario the polarization mechanism and quenching mechanism are two independent processes. Recent results[39,40] in the literature on the influence of molecular oxygen on the nitroxide CW EPR spectrum may be relevant to this hypothesis. Experimentally it is found that the EPR spectrum of TEMPO "disappears" as the concentration of molecular oxygen is increased.[39] It is proposed that this is not due to broadening of the EPR spectrum, but the actual formation of a diamagnetic "complex".[40] It is plausible that the reversible formation of this "complex" is the source of polarization.

Conclusions

We have confirmed that the absorptive CIDEP of nitroxides in the presence of oxygen, as demonstrated by Obi,[9] is caused by singlet oxygen, because the decay time of the nitroxide spin polarization correlates directly with the lifetime of singlet oxygen (measured by phosphorescence). In addition, a deuterium isotope effect on the spin polarization decay time was observed, which is a signature of singlet oxygen involvement. The spin polarization intensity of the nitroxide is determined by the rate constants and concentrations in a complex competing reaction mechanism (Scheme 1), where the concentrations of nitroxide and oxygen are critical. By using isotope labeled nitroxides (^{15}N, ^{14}N), the relative spin polarization efficiencies of TEMPO, O-TEMPO, and OH-TEMPO were determined. Although the quenching rate constant of singlet oxygen by O-TEMPO is higher than that by TEMPO and OH-TEMPO, the observed net absorptive spin polarization intensities are approximately equal, showing that also other processes in addition to the quenching rate constant govern the spin polarization efficiency of nitroxides by singlet oxygen.

Acknowledgment. We thank the National Science Foundation for their financial support (grant CHE-01-10655).

References and Notes

(1) Blaettler, C.; Jent, F.; Paul, H. *Chem. Phys. Lett.* **1990**, *166*, 375.
(2) Kawai, A.; Okutsu, Obi, K. *J. Phys. Chem.* **1991**, *95*, 9130.
(3) Kawai, A.; Obi, K. *J. Phys. Chem.* **1992**, *96*, 52.
(4) Kawai, A.; Obi, K. *J. Phys. Chem.* **1992**, *96*, 5701.
(5) Turro, N. J.; Khudyakov, I. V.; Bossmann, S. H.; Dwyer, D. W. *J. Phys. Chem.* **1993**, *97*, 1138.
(6) Goudsmit, G.-H.; Paul, H.; Shushin, A. I. *J. Phys. Chem.* **1993**, *97*, 13243.
(7) Kobori, Y.; Kawai, A.; Obi, K. *J. Phys. Chem.* **1994**, *98*, 6425.
(8) Kobori, Y.; Takeda, K.; Tsuji, K.; Kawai, A.; Obi, K. *J. Phys. Chem. A* **1998**, *102*, 5160.
(9) Mitsui, M.; Takeda, K.; Kobori, Y.; Kawai, A.; Obi, K. *Chem. Phys. Lett.* **1996**, *262*, 125.
(10) Kawai, A.; Mitsui, M.; Kobori, Y.; Obi, K. *Appl. Magn. Reson.* **1997**, *12*, 405.
(11) Fujisawa, J.; Ohba, Y.; Yamauchi, S. *J. Phys. Chem A* **1997**, *101*, 434.
(12) Kawai, A. *Appl. Magn. Reson.* **2003**, *23*, 349.
(13) Mitsui, M.; Takeda, K.; Kobori, Y.; Kawai, A.; Obi, K. *J. Phys. Chem. A* **2004**, *108*, 1120.
(14) Khan, A. U.; Kasha, M. *Proc. Natl. Acad. Sci. U.S.A.* **1979**, *76*, 6047.
(15) Klemchuk, P. P.; Gande, M. E. *Makromol. Chem., Macromol. Symp.* **1989**, *28*, 117.

(16) Denisov, E. T. *Polym. Degrad. Stab.* **1991**, *34*, 325.
(17) Hepp, M. G.; Kramer, H. E. A. *J. Photochem. Photobiol., A* **1994**, *78*, 19.
(18) Heller, H. J.; Blattmann, H. R. *Pure Appl. Chem.* **1973**, *36*, 141.
(19) Step, E. N.; Turro, N. J.; Gand, M. E.; Klemchuk, P. P. *Macromolecules* **1994**, *27*, 2529.
(20) Jockusch, S.; Liu, Z.; Ottaviani, M. F.; Turro, N. J. *J. Phys. Chem. B* **2001**, *105*, 7477.
(21) Jockusch, S.; Dedola, G.; Lem, G.; Turro, N. J. *J. Phys. Chem. B* **1999**, *103*, 9126.
(22) Koptyug, I. V.; Ghatlia, N. D.; Sluggett, G. W.; Turro, N. J.; Ganapathy, S.; Bentrude, W. G. *J. Am. Chem. Soc.* **1995**, *117*, 9486.
(23) Belford, R. E.; Seely, G.; Gust, D.; Moore, T. A.; Moore, A.; Cherepy, N. J.; Ekbundit, S.; Lewis, J. E.; Lin, S. H. *J. Photochem. Photobiol., A* **1993**, *70*, 125.
(24) Darmanyan, A. P.; Tatikolov, A. S. *J. Photochem.* **1986**, *32*, 157.
(25) Hyde, J. S.; Subczynski, W. K. Spin-Label Oximetry. In *Biological Magnetic Resonance. Spin Labeling*: *Theory and Applications*; Berliner, L. J., Reuben, J., Eds.; Plenum Press: New York, 1989; Vol. 8.
(26) Molin, Y.; Salikhov, K. M.; Zamaraev, K. I. *Spin Exchange*; Springer-Verlag: Berlin, Germany, 1980.
(27) Goudsmit, G.-H.; Paul, H. *Chem. Phys. Lett.* **1993**, *208*, 73.
(28) Wilkinson, F.; McGarvey, D. J.; Olea, A. F. *J. Am. Chem. Soc.* **1993**, *115*, 12144.
(29) Murov, S. L.; Carmichael, I.; Hug, G. L. *Handbook of Photochemistry*, 2nd ed.; Marcel Dekker: New York, 1993.
(30) Stevens, B.; Marsh, K. L.; Barltrop, J. A. *J. Phys. Chem.* **1981**, *85*, 3079.
(31) Olea, A. F.; Wilkinson, F. *J. Phys. Chem.* **1995**, *99*, 4518.
(32) Schmidt, R.; Afshari, E. *Ber. Bunsen-Ges. Phys. Chem.* **1992**, *96*, 788.
(33) Stevens, B.; Perez, S. R.; Ors, J. A. *J. Am. Chem. Soc.* **1974**, *96*, 6846.
(34) Rodgers, M. A. J. *J. Am. Chem. Soc.* **1983**, *105*, 6201.
(35) Ogilby, P. R.; Foote, C. S. *J. Am. Chem. Soc.* **1983**, *105*, 3423.
(36) Hurst, J. R.; Schuster, G. B. *J. Am. Chem. Soc.* **1983**, *105*, 5756.
(37) Scaiano, J. C.; Connolly, T. J.; Mohtat, N.; Pliva, C. N. *Can. J. Chem.* **1997**, *75*, 92.
(38) Keith, A.; Horvat, D.; Snipes, W. *Chem. Phys. Lipids* **1974**, *13*, 49.
(39) Vorob'ev, A. Kh.; Chernova, D. A.; Gurman, V. S. *Russ. J. Phys. Chem.* **2004**, *78*, 55.
(40) Barton, D. H.; Le Gloahec, V. H.; Smith, J. *Tetrahedron Lett.* **1998**, *39*, 7483.